An Finite Element Analysis of Patellar and Quadriceps Tendon Injury during Squatting

Bo-Yu Huang (黃柏喻), Eduardo Marco Hsu (徐子評), Chi-Lun Lin(林啟倫)

Abstract

Squatting is one of the most fundamental exercises among sports. However, heavy loadings or improper posture may lead to severe injury at the knee, more specifically at the quadriceps tendon. The majority of in vivo and in vitro finite element analysis studies regarding the effects of weightlifting on the knee revolves around subjects who are very familiar to high intensity exercises. Little has been discussed about the effects of squatting on the knee on the average man. Our objective is to find the effects of squatting on the average man that does not frequent in intense exercise. Two different approaches were taken. One method consists of recreating a computational 3D model of an MRI of a healthy male's knee and, through finite element analysis (FEA), solve for internal loadings by adding appropriate boundary conditions and material coefficients. The other method dwells on capturing subjects squatting with motion capture video and analyzing the kinematics and kinetics data involved in the exercise. Both manners serve as reciprocal validation.

Keywords: patellar tendon, squatting, patellar tendon properties, finite element analysis of knee and inverse dynamics of knee.

1. Introduction

Weightlifting became more widespread recently and was acknowledged as an enhancement to other sport competition. Being able to fully control muscle groups and maximizing one's strength not only improves one's health but also brings competitive advantage to professional athletes. This type of training is called cross-training which can improve performance of the targeted sport. Weightlifting was first included in the Olympics as an individual competition in 1896 and it became much more popular through the 20th century. The main purpose of this type of training is to increase performance and prevent potential injury such as ankle sprain or jumper's knee. However, weightlifting itself contains risks. Wrong posture, overestimating one's ability and having insufficient rest time can all lead to severe injury.

Nevertheless, injuries occur with high frequency in weight training, many during squatting. While squatting, the main muscle groups used are the upper shoulder, biceps, abdominal muscles, thigh and hamstring. Almost the entire body is engaged with the activity. Certain injuries occur, such as bony tissue or soft tissue [19]. The maximum knee extensor moment is different due to size of the trunk. To eliminate this factor, exclusion of the subjects who are professional weightlifting competitors is necessary. Tendon injury includes both acute and chronic. Tendinopathy chronic injury accounted for 12-25% [24] of all strength training injuries. Patellar and quadriceps tendon are usually taken into consideration. For acute tendon injury, as Mark mentioned [24], tendon

rupture is much relevant to the overloading of the tendon rather than the slight dislocation of the articulated joint. For chronic tendon injury, rest time and loading are the two major roles. Since no advanced research clearly defined the adequate resting time in relation to injury, as subject variation exists, our research focus on acute tendon injury, specifically, patellar and quadriceps tendon.

The method of using free body diagram and Newton Euler equation is applied to find the patellofemoral joint reaction force (PFJR) [32]. In order to define PFJR, quadriceps muscle force and flexion are needed. The approach [42] collected cinematographic data of patellar tendon rupture of a weightlifting championship. A motion capture camera was utilized to record both kinematic and kinetic data, and modelling it into simple planar motion consisting of five linkages. Next, the method of "inverse dynamics" was later widely recognized after the publication of *Biomechanics and motor control of human movement* [39], which deeply analyzes the human gait (0.014 seconds per frame). With the help of force plates, researchers are able to calculate the force and moment applied on the knee joint.

In the past, scientists knew how to effectively gather the geometry and data of the patellar tendon using advanced techniques such as magnetic resonance image (MRI) or clinical tomography (CT), the first of experiment on the tensile strength of patellar tendon were mostly based on cadavers [6]. However, most of the bodies were rejected due to contamination, medical history of the donor and other clinical concerns. This method took into account sex, age and exercise habits of the donors. Some scientists may use ANCOVA to minimize the discrepancy among them [4]. Customized contacting extensometer measurement was put into use of cyclic loading and measurement. The concept of viscoelasticity was also widely implemented into the data curve fitting.

Later on, not until 2003 [31], a study made use of ultrasound image and EMG combined with a dynamometer, which was mimicked by many researchers later on. They tested the biomaterial properties which was aimed at finding the force, stiffness and deformation, all essential in finite element model analysis. For instance, there are studies [29] about the relationship between the tendon force and tendon deformation under slow or fast ramped contraction. The fundamental idea is that quadriceps and hamstring are antagonistic muscle to the knee joint. The co-contraction torque is put to maintain the joint rigidity. For example, EMG is designed to collect the force of hamstring. Ultrasound image is aimed at finding the instant deformation of target tissue. Dynamometer is put to read the knee extensor load which antagonist to the hamstring (knee flexor load).

Nowadays, researches on the lower-limb three-dimensional reconstruction are numerous, focusing on the necessity of whether a full knee replacement is needed or just the repair of certain soft tissues. Considering cartilage [12], the material properties including deformable or rigid body were both considered. To test the validation of the total knee arthroplasty (TKA) [40], they collected 15 cadaveric subjects for the force experimental data and compared the output result with the simulation model. The validation of our model will be

achieved by the comparison between the output from the computational model and the experimental value calculated through inverse dynamics. Validation always comes prior to the research and simulation [30]. They assume cartilage and meniscus are linearly elastic, and ligament as hyperelastic which show great similarity with previous experiments regarding human gait load.

In DA Winter's publication [39] about rigid body analysis of the lower limb during human gait, which segments body parts (foot, tibia, femur) into linkages and, by setting input reactive forces and position angles, interacting joint forces and moments can be solved. Even the energy method corresponds with the same kinematic results. We applied this concept into our model. After inputting tibia force into the three dimensional model, the final stresses the tendons support can be determined.

The relevance of computational modelling in this study serves to simulate the internal forces that may cause failure in the patellar and quadriceps tendon during squatting. Conclusion made from previous studies [15], during weightlifting, the maximum compressive forces and stresses in the retropatellar occurs near or while bending at 90° angle. Therefore, two positions relevant to the knee geometry were chosen for the MR imaging: at rest, straight at a 180° angle and flexion angle at a 90° angle. After creating three-dimensional models, we may apply boundary conditions and input forces from the motion capture experiment into *Abaqus*, to simulate all internal stresses in the knee.

Our purpose is to focus on the relationship between weightlifting and both patellar and quadriceps tendon. Some studies have done this before [8]. They used *Slicematic*, *Hypermesh* and *Abaqus* to build up the knee joint model. In our computational approach, the medical image processing differs from theirs in that we used *Mimics* instead of *Slicematic*. Majority of the bibliography compared non-injured subjects and subjects with particular past injuries in order to distinguish the difference between two control groups.

2. Method

2.1. MRI resource

The main goal is to identify the maximum loading of the patellar tendon for squatting in the average males. However, this is almost impossible to test out without a great chance of injury, so we resort to the finite element analysis. To build our model, first, MRI scan of a healthy 22 years old male's (Bo-Yu Huang) knee at the Instrument Technology Research Center (ITRC) located in Shinchu, Taiwan. The range of the scan is from the femoral shaft to the tibial shaft, in two different knee positions: straight and flexion angle of 90 degrees. The CT and MRI blocks consisted of parallel digital images separated at intervals of 1.5 mm. in the sagittal, coronal and axial planes with the knee at 0° and 90° flexion.

2.2. Subjects

After approved by the Institutional Review Board (IRB), we recruited 10 voluntary males performing squat. Subjects' age was around 18 to 26. All subjects do moderate intensity exercise at least three times a week, each time for at least thirty minutes. The average weight and the average height of ten subjects are 74.3 kg and 1.74 meters, respectively. The weight of squatting

divided into three categories: bilateral self-squatting, empty bar (5.3 kilograms) and two 10 lb. plates (approximately 14 kg). Participants were asked to perform in a very slow motion during bilateral squatting in order to approximate acceleration nearly zero.

2.3. Facility

ExpertVision Motion Analysis System (Motion Analysis Corp., Santa Rosa, CA) and two force plates (Kistler, Winterthur, Switzerland type 9865B) were used to collect the kinematics and kinetics data. Force plate gather the ground reaction force. Markers of 25 mm. in diameter were put on the joint including hip, knee (2) ankle (2), toe (2), heel, clavicle, C5 and sternum for the kinematics data. All squatting experiments were conducted in the laboratory of Dr. Fong-Chin Su, Deputy Minister of Ministry of Science in Taiwan. The squatting bar and bar pieces belonged to Yu Xuan Wu.

3. Assumption

An assumption of the experimental approach is that the motion is quasi-static, meaning that the velocities are kept as minimal as possible so as to neglect any acceleration. This method can be proved by kinematics data of the tracker on human body (as acceleration almost approaches zero). Furthermore, since the movement in the direction normal to the coronal plane is approximately zero when the knee flexion angle is around 90 degrees while squatting, the motion of the lower limb can be simulated as two dimensional. These two concepts are utilized in inverse dynamics calculation in order to gather the input force and boundary conditions in the finite element analysis.

Moreover, another assumption is that, during squatting, ligaments play a least important role in maintaining the rigidity of the knee joint. The majority of the force comes from compression, which means that ligaments such as ACL and PCL that tend to bear tension are of little use [43]. The loading comes from the upper body and causes vertical force which results in ground reaction force. The primary concern is to study the patellar and quadriceps tendon, rather than figuring out every detail of the knee joint.

4. Squatting experiments

Lower extremity kinematics were collected using eight-camera motion analysis system at 100 frames per second and the maximum tracking speed is 300 mm. per frame. Trackers include hip, knee (2) ankle (2), toe (2) in order to form the center of revolute joint. Ground reaction forces were recorded at 1000 Hz. Subjects were asked to step a foot on separate force plates. The confirmation of equal force applied on the force plate is essential. However, force data recorded from the force plates was not accurate enough. Nonetheless, our focus was narrowed down to one leg. “Inverse dynamics” method was then utilized on the right leg and two dimensional analysis. The capture duration was 8 seconds per squat.

After all the force plate data and the marker footage was collected, the files were imported into Cortex (*Cortex-64 3.0.0.1271*). The markers were labeled and links were drawn for a better visualization of the squatting gait. See Figure 1. TRC files were exported for the extraction of position coordinates, that were later used for the inverse dynamics method.

5. FE Model construction

MR images saved in DICOM format were processed with Mimics Innovation Suite 16.0 Materialise. See Figure 2.

After construction of the model, elements were isolated and saved as independent models (patellar tendon, quadriceps tendon, meniscus, patella, femur, tibia, cartilage). Each model was then refined and smoothed in *Geomagic Studio 12 (Geomagic Inc., Research Triangle Park,Morrisville, NC, USA).* Later on, the models were then meshed at higher quality in *Hypermesh 13.0 (Altair Engineering Corp)* until the quality index (QI) was zero. Otherwise, the model must be saved and smoothed once again in *Geomagic*, and meshed in *Hypermesh* until quality index reaches zero. Tria mesh size was 0.5 near contact surfaces and boundaries. In order to decrease the number of elements in the model (so as to reduce the calculation time in Abaqus), meshing of the tibia and the femur increased gradually at 0.5 intervals until 2, from the head of the bones to the center of the bone section. Material and properties were assigned according to existing literature.

Once the surface meshing was finalized, we tetrameshed the model. See Figure 3. The contact surfaces between the 3D components were found in *Hypermesh* with a proximity distance of 0.01 and individual properties were assigned to each individual contact pair. See Figure 4. Material properties are shown in Table 2.

6. Boundary conditions

The boundary conditions in the model consist of two fixed ends and a load. Three sets were created by selecting elements on the quadriceps tendon, femoral shaft and tibial shaft surfaces. For the fixed ends (quadriceps tendon and femoral shaft) two load collectors with constraints of six degrees of freedom were created. The loading force vector obtained from the experimental trials was set at the tibial shaft in the z direction.

7. Model simulation

The model from *Hypermesh* was imported into *Abaqus*. A local coordinate system was selected for each element. By creating sets at the cross-sectional area at the femur, quadriceps tendon and patellar tendon, we were able to probe for the reaction force at the given areas. Jobs were submitted in order to find the reaction force at the fixed ends. The same iteration was done for the rest of experimental data.

8. Results

The input force from the ground reaction force was set at the tibial shaft in the z direction while the femoral shaft and quadriceps tendon were kept fixed for all six degrees of freedom. Then, we solved for the projection of the knee to hip force vector and compared the values to the results calculated from the inverse dynamics method. The results are shown in Figure 5. Values of the force vectors from the model and inverse dynamics are shown in Table 3.

From the animation of the model in *Abaqus*, we observed a major displacement of the tibial shaft in the sagittal plane, where most of the deformation belonged to the patellar tendon, as seen in Figure 7. The error percentage of each subject is shown in Figure 8.

9. Discussion

9.1. Posture

The squatting posture of the subjects was only restricted so that the feet stayed within the force plate. Other factors such as width between feet, angle on transverse plane between foot and sagittal plane, instability of knees, lifting of heel from force plate, depth of squat, among others, were not limited. For a more precise study, there should be more restrictions regarding the squatting posture, thus reducing the number of variables regarding posture that will affect the results.

A direct issue with the unrestricted squat was the position. The total number of subjects studied was originally 10 but it had to be reduced to 9 because one subject did not reach a 90° squat position, so no relevant data could be obtained from that subject. The knee angle was verified from the TRC file exported from *CORTEX*.

9.2. Force plate

The force plate responsible of recording the ground reaction force was found to be imprecise for the data collected. However, redoing the experiment was not a viable option since not all subjects were going to be available for a second trial. Thus, the ground reaction force of our study was compromised. Despite this, we still utilized the input force Regarding the imprecision of the force plate, we contacted the supervisor at Dr. Fong-Chin Su's Motion Laboratory regarding these imprecisions and it was later found that there was indeed a glitch in the force plate.

9.3. Model compatibility

The 3D model created belongs to Bo-Yu Huang, whose height is 182 cm. and body weight is 60kg. Subject a and I were the most similar to Bo-Yu's body type. However, there is a great difference in error percentage. Upon further inspection of their squatting gaits in *Cortex*, subject i's squat is more fluid and smooth in comparison to subject a. Subject a, on the other hand, squats in a more segmented and there were signs of knee instability when maximum bending of the knee was reached.

10. Conclusion

An overlooked assumption was the fact that the quadriceps muscle has a direct impact on the quadriceps tendon, which means that there should be an input source (such as an EMG signal) at the quadriceps tendon in order to balance the moment caused by input force.

Since there was no input value at the quadriceps tendon, most of the force was absorbed by the cartilaginous tissue seen at Figure 7 bottom, resulting in the failure of these tissues.

11. Reference

[1] Adouni, M. and A. Shirazi-Adl (2009). "Knee joint biomechanics in closed-kinetic-chain exercises." Computer methods in biomechanics and biomedical engineering 12(6): 661-670.

[2] Ashman, R., et al. (1984). "A continuous wave technique for the measurement of the elastic properties of cortical bone." Journal of biomechanics 17(5): 349-361.

[3] Beillas, P., et al. (2004). "A new method to investigate in vivo knee behavior using a finite element model of the lower limb." Journal of biomechanics 37(7): 1019-1030.

[4] Chandrashekar, N., et al. (2012). "Effects of cyclic loading on the tensile

properties of human patellar tendon." The knee 19(1): 65-68.

[5] Chowdhury, S. and N. Kumar (2013). "Estimation of forces and moments of lower limb joints from kinematics data and inertial properties of the body by using inverse dynamics technique." Journal of Rehabilitation Robotics 1(2): 93-98.

[6] Cooper, D. E., et al. (1993). "The strength of the central third patellar. tendon graft A biomechanical study." The American Journal of Sports Medicine 21(6): 818-824.

[7] Donahue, T. L. H., et al. (2003). "How the stiffness of meniscal attachments and meniscal material properties affect tibio-femoral contact pressure computed using a validated finite element model of the human knee joint." Journal of biomechanics 36(1): 19-34.

[8] Farrokhi, S., et al. (2011). "Individuals with patellofemoral pain exhibit greater patellofemoral joint stress: a finite element analysis study." Osteoarthritis and Cartilage 19(3): 287-294.

[9] Fekete, G., et al. (2014). "Patellofemoral model of the knee joint under non-standard squatting." Dyna 81(183): 60-67.

[10] Halonen, K., et al. (2013). "Importance of depth-wise distribution of collagen and proteoglycans in articular cartilage—a 3D finite element study of stresses and strains in human knee joint." Journal of biomechanics 46(6): 1184-1192.

[11] Halonen, K., et al. (2016). "Importance of patella, quadriceps forces, and depthwise cartilage structure on knee joint motion and cartilage response during gait." Journal of biomechanical engineering 138(7): 071002.

[12] Halloran, J. P., et al. (2005). "Explicit finite element modeling of total knee replacement mechanics." Journal of biomechanics 38(2): 323-331.

[13] Hansen, P., et al. (2006). "Mechanical properties of the human patellar tendon, in vivo." Clinical Biomechanics 21(1): 54-58.

[14] Harris, M. D., et al. (2016). "A Combined Experimental and Computational Approach to Subject-Specific Analysis of Knee Joint Laxity." Journal of biomechanical engineering 138(8): 081004.

[15] Hartmann, H., et al. (2013). "Analysis of the load on the knee joint and vertebral column with changes in squatting depth and weight load." Sports medicine 43(10): 993-1008.

[16] Hashemi, J., et al. (2005). "The mechanical properties of the human patellar tendon are correlated to its mass density and are independent of sex." Clinical Biomechanics 20(6): 645-652.

[17] Hayes, W. and L. Mockros (1971). "Viscoelastic properties of human articular cartilage." Journal of applied physiology 31(4): 562-568.

[18] Heegaard, J., et al. (2001). "A computer model to simulate patellar biomechanics following total knee replacement: the effects of femoral component alignment." Clinical Biomechanics 16(5): 415-423.

[19] Joseph, S. Y. and P. A. Habib (2005). Common injuries related to weightlifting: MR imaging perspective. Seminars in musculoskeletal radiology,

Publishers, Inc., 333 Seventh Avenue, New York, NY 10001, USA.

[20] Kiapour, A., et al. (2014). "Finite element model of the knee for investigation of injury mechanisms: development and validation." Journal of biomechanical engineering 136(1): 011002.

[21] Kłodowski, A., et al. (2016). "Merge of motion analysis, multibody dynamics and finite element method for the subject-specific analysis of cartilage loading patterns during gait: differences between rotation and moment-driven models of human knee joint." Multibody System Dynamics 37(3): 271-290.

[22] Kongsgaard, M., et al. (2010). "Fibril morphology and tendon mechanical properties in patellar tendinopathy effects of heavy slow resistance training." The American Journal of Sports Medicine 38(4): 749-756.

[23] Kubo, K., et al. (2001). "Effects of isometric training on the elasticity of human tendon structures in vivo." Journal of applied physiology 91(1): 26-32.

[24] Lavallee, M. E. and T. Balam (2010). "An overview of strength training injuries: acute and chronic." Current sports medicine reports 9(5): 307-313.

[25] Li, G., et al. (2001). "Variability of a three-dimensional finite element model constructed using magnetic resonance images of a knee for joint contact stress analysis." Journal of biomechanical engineering 123(4): 341-346.

[26] Moreira, P., et al. (2013). Biomechanical models for human gait analyses using inverse dynamics formulation. 5º Congresso Nacional de Biomecânica, Sociedade Portuguesa de Biomecânica.

[27] O'Brien, T. D., et al. (2010). "Mechanical properties of the patellar tendon in adults and children." Journal of biomechanics 43(6): 1190-1195.

[28] Onambélé, G. N., et al. (2007). "Gender-specific in vivo measurement of the structural and mechanical properties of the human patellar tendon." Journal of orthopaedic research 25(12): 1635-1642.

[29] Pearson, S. J., et al. (2007). "Creep and the in vivo assessment of human patellar tendon mechanical properties." Clinical Biomechanics 22(6): 712-717.

[30] Pena, E., et al. (2006). "A three-dimensional finite element analysis of the combined behavior of ligaments and menisci in the healthy human knee joint." Journal of biomechanics 39(9): 1686-1701.

[31] Reeves, N. D., et al. (2003). "Effect of strength training on human patella tendon mechanical properties of older individuals." The Journal of physiology 548(3): 971-981.

[32] Reilly, D. T. and M. Martens (1972). "Experimental analysis of the quadriceps muscle force and patello-femoral joint reaction force for various activities." Acta Orthopaedica Scandinavica 43(2): 126-137.

[33] Rho, J. Y., et al. (1993). "Young's modulus of trabecular and cortical bone material: ultrasonic and microtensile measurements." Journal of biomechanics 26(2): 111-119.

[34] Smith, S. M., et al. (2008). "Tibiofemoral joint contact forces and

knee kinematics during squatting." Gait & posture 27(3): 376-386.

[35] Svensson, R. B., et al. (2012). "Mechanical properties of human patellar tendon at the hierarchical levels of tendon and fibril." Journal of applied physiology 112(3): 419-426.

[36] Wang, J., et al. (2014). "Modelling and Analysis on Biomechanical Dynamic Characteristics of Knee Flexion Movement under Squatting." The Scientific World Journal 2014.

[37] Wang, Y., et al. (2014). "Comparison of stress on knee cartilage during kneeling and standing using finite element models." Medical engineering & physics 36(4): 439-447.

[38] Wilson, T. W., et al. (1999). "A biomechanical analysis of matched bone-patellar tendon-bone and double-looped semitendinosus and gracilis tendon grafts." The American Journal of Sports Medicine 27(2): 202-207.

[39] Winter, D. A. (2009). Biomechanics and motor control of human movement, John Wiley & Sons.

[40] Woiczinski, M., et al. (2016). "Development and validation of a weight-bearing finite element model for total knee replacement." Computer methods in biomechanics and biomedical engineering 19(10): 1033-1045.

[41] Wu, G., et al. (2002). "ISB recommendation on definitions of joint coordinate system of various joints for the reporting of human joint motion—part I: ankle, hip, and spine." Journal of biomechanics 35(4): 543-548.

[42] Zernicke, R. F., et al. (1977). "Human patellar-tendon rupture." J Bone Joint Surg Am 59(2): 179-183.

[43] 林惠芬, et al. (2001). “步態雙之撐期下肢肌力的預測”. 館藏成大圖書館

12. Acknowledgements

Institutional review board (IRB) affiliated to National Cheng Kung University of Medical division approved our project. Any sort of human experiment proceduremust be approved by the IRB commetee. MRI DICOM file were acquired through the help of Narlab. Our squatting experiment was conducted in the Motion Laboratory of Dr. Fong-Chin Su, professor in National Cheng Kung University of department of Medical Engineering and also the Deputy Minister of Ministry of Science in Taiwan. All equipment including motion capture system and forceplate belong to the Motion Lab.

13. Tables

Acquired data					
	Age	Height (cm)	Weight (kg)	Empty bat (kg)	Bar + 2 plates (kg)
A	20	172	60	65.3	74.37
B	22	173	68	73.3	82.37
C	21	178	93	98.3	107.37

D	20	172	78	83.3	92.37
E	22	174	82	87.3	96.37
F	20	187	84	89.3	98.37
G	20	169	72	77.3	86.37
H	22	170	70	75.3	84.37
I	20	172	62	67.3	76.37

Assumption data					
	Age	Foot weight (kg)	Shank weight (kg)	Thigh weight (kg)	Single forceplate without bar (N)
A	20	0.87	2.8	6	294.3
B	22	0.99	3.16	6.8	333.54
C	21	1.35	4.3	9.3	456.16
D	20	1.13	3.6	7.8	382.6
E	22	1.19	3.8	8.2	402.2
F	20	1.22	3.9	8.4	412
G	20	1.04	3.3	7.2	353.2
H	22	1.02	3.3	7	342.3
I	20	0.9	2.9	6.2	304.1

*Table 1: Subject data collected and assumed. Note: foot weight = 0.0145*Weight, Shrank weight = 0.0465*Weight, Thigh weight = 0.1*Weight (according to DA Winter 2009)*

Component	Density	Young's Modulus	Poisson Ratio	Shear Modulus
Quadriceps tendon		$E_1 = 4.75$	$\nu_{12} = 0.25$	$G_{12} = 1.1$
		$E_2 = 4.75$	$\nu_{13} = 0.022$	$G_{13} = 45.64$
		$E_3 = 10$	$\nu_{23} = 0.022$	$G_{23} = 45.64$
Patellar tendon		$E = 5$	$\nu = 0.46$	
Tibial/femoral/patellar cartilage		$E = 15$	$\nu = 0.475$	
Meniscus	1.5×10^{-9}	$E_1 = 20$	$\nu_{12} = 0.2$	$G_{12} = 1.1$
		$E_2 = 140$	$\nu_{13} = 0.3$	
		$E_3 = 20$	$\nu_{23} = 0.2$	
Tibia/femur	1.817×10^{-9}	$E_1 = 12000$		$G_{12} = 4530$
		$E_2 = 13400$		$G_{13} = 5610$
		$E_3 = 20000$		$G_{23} = 6230$
Patella	2×10^{-9}	$E = 15000$	$\nu = 0.3$	

Table 2: Material properties of soft tissue and bone in finite element model

	Theoretical solution	Numerical solution
	Scalar	Scalar
A_w	161.8546591	137.4841215
B_w	183.4352803	197.9549617
C_w	250.8747216	187.7485955
D_w	210.4110568	185.1470798
E_w	221.2013674	191.3609117
F_w	226.5965227	206.429667
G_w	194.2255909	202.2366914
H_w	188.8304356	185.1649084
I_w	167.2498144	167.1972423
A_w+b	185.9765985	165.6837604
B_w+b	208.7608679	210.3312895
C_w+b	279.9617096	233.8415372
D_w+b	237.2412045	202.3208611
E_w+b	248.6333392	206.5856248
F_w+b	254.3294065	251.1580544
G_w+b	220.1530025	220.9954366
H_w+b	214.4569352	235.2969778
I_w+b	191.6726659	191.4691742
A_w+b+p	203.2428952	193.2816295
B_w+b+p	225.1051977	228.5197961
C_w+b+p	293.424893	260.9239943
D_w+b+p	252.4330758	220.6594023
E_w+b+p	263.3642271	240.4681817
F_w+b+p	268.8298027	292.1422385
G_w+b+p	236.036349	235.4022121
H_w+b+p	230.5707733	292.8152996
I_w+b+p	208.7084708	208.5382004

Table 3: Raw data of theoretical solution from Abaqus and numerical solution from inverse dynamics

14. Figures

Figure 1: Thresholding in Mimics

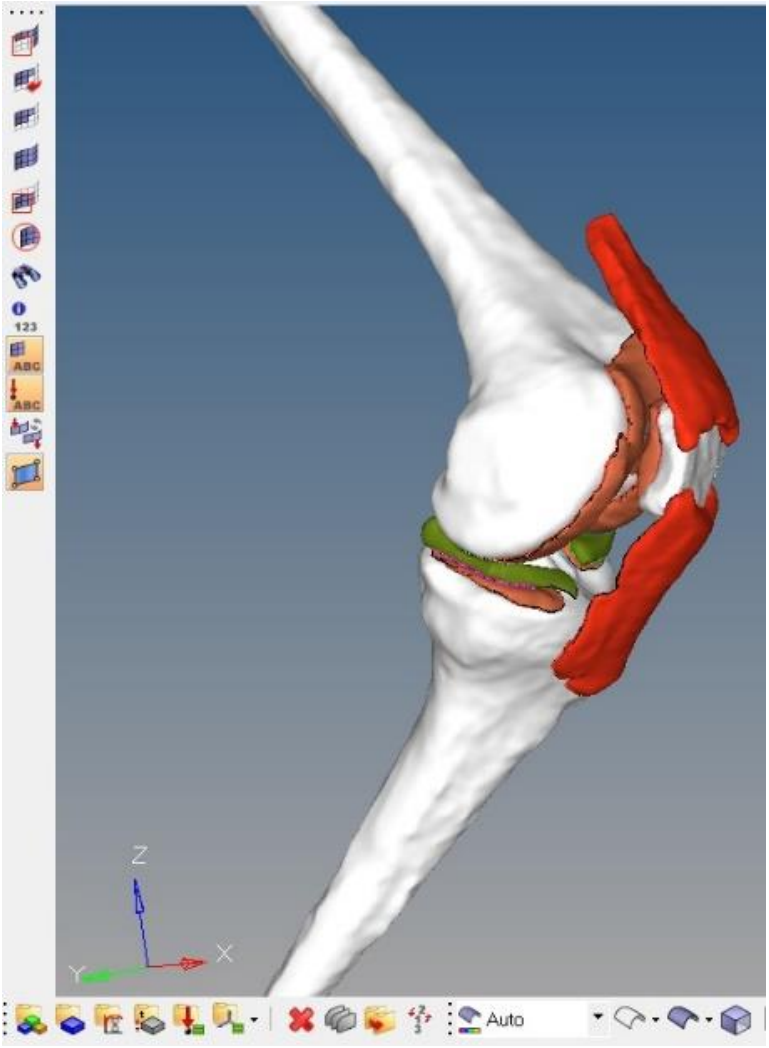

Figure 2: Tetrameshing in Hypermesh

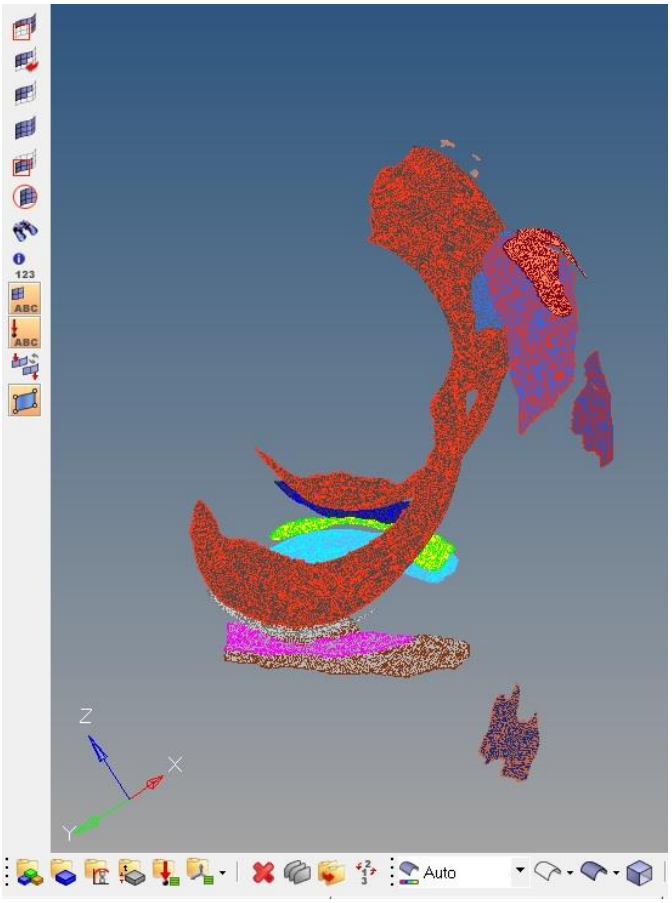

Figure 3: Contact pair found in 90 degree knee model

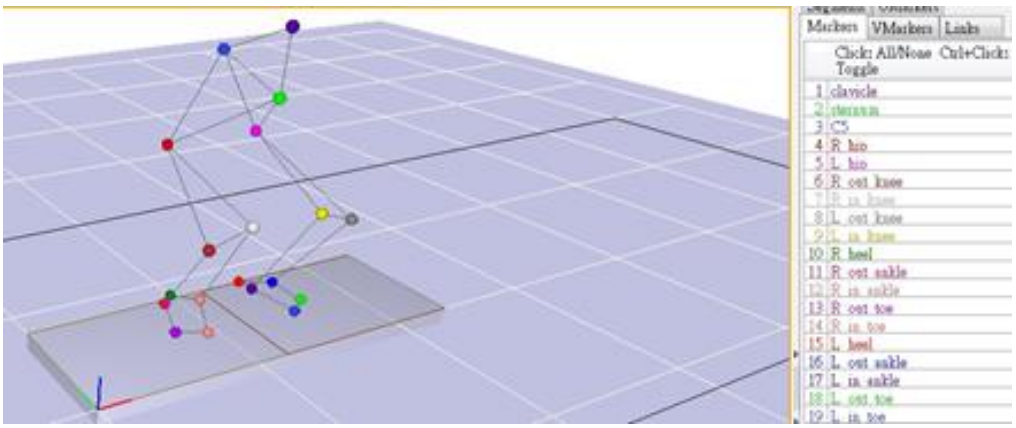

Figure 4: Identifying markers in Cortex

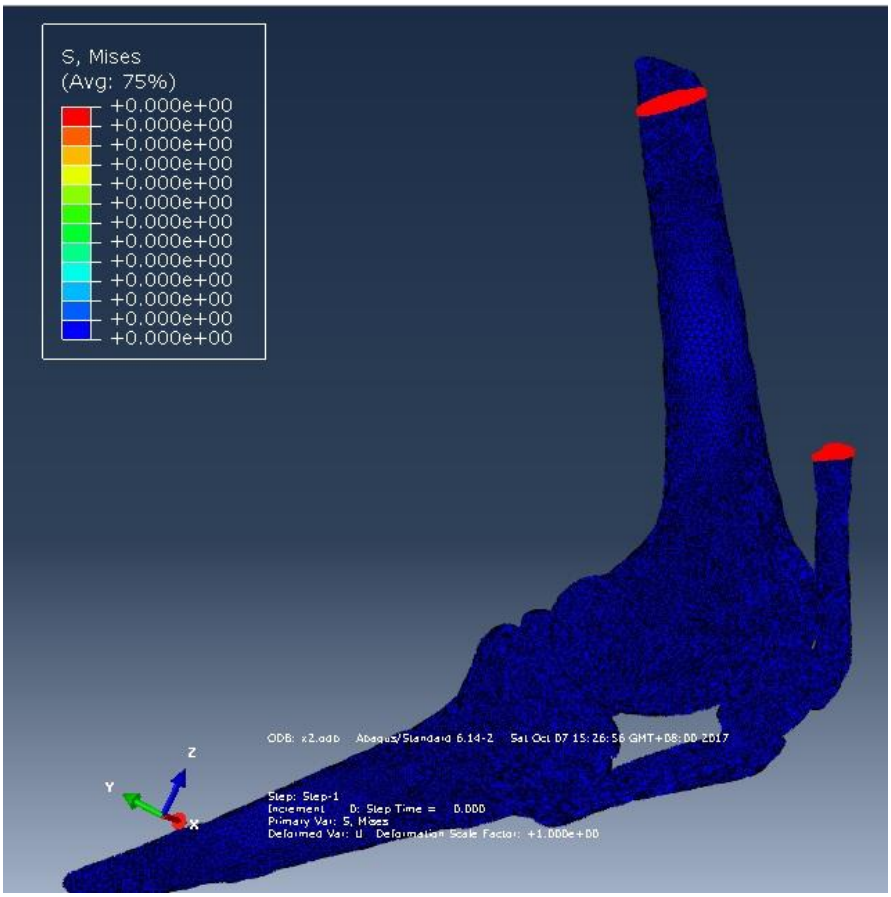

Figure 5: 3D model in Abaqus showing reaction forces at femur and quadriceps tendon

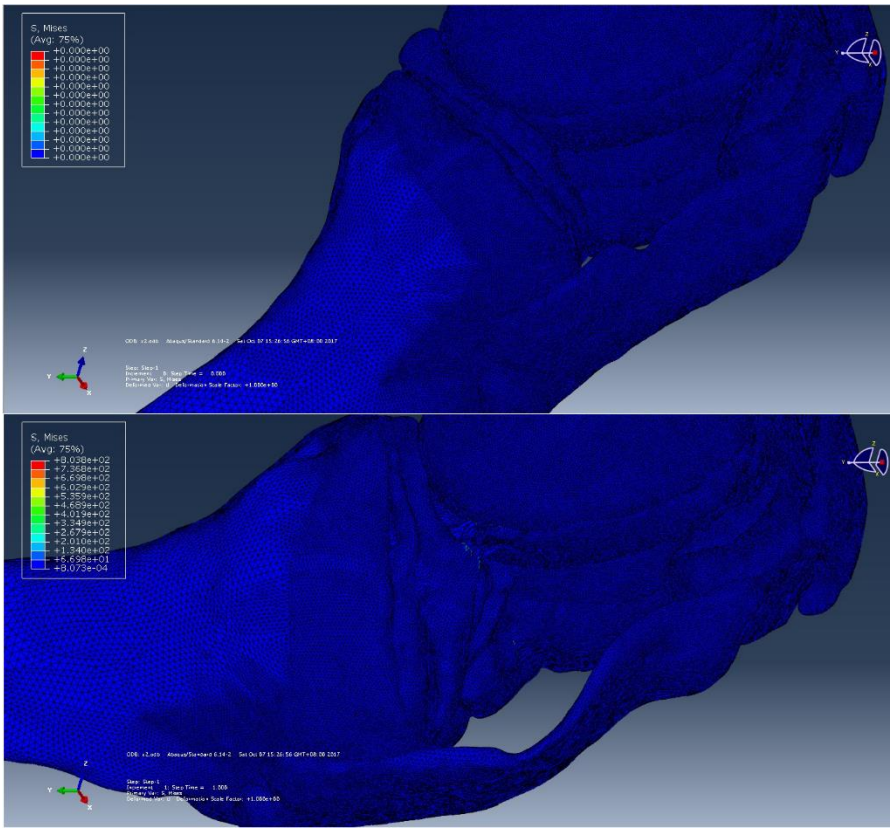

Figure 7: Animation in Abaqus before (top) and after (bottom) deformation.

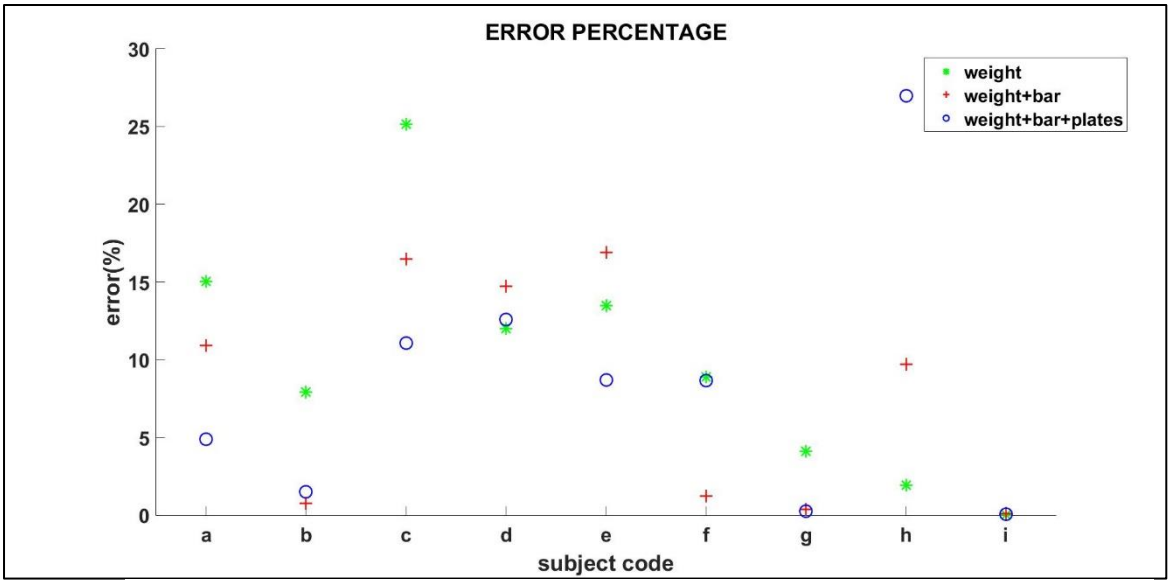

Figure 8: Percentage error of output simulation compared to experimental values for 9 subjects